Long-time stable HTSC DC-SQUID gradiometers with silicon dioxide passivation for measurements with superconducting flux transformers

P Seidel[1], C Becker[1], A Steppke[1], M Buettner[1], H Schneidewind[2], V Grosse[1], G Zieger[1] and F Schmidl[1]

[1] Institut für Festkörperphysik, Friedrich-Schiller-Universität Jena, Helmholtzweg 5, D-07743 Jena, Germany
[2] Institut für Photonische Technologien (IPHT) e.V., Albert-Einstein-Straße 9, D-07745 Jena, Germany
paul.seidel@uni-jena.de

Abstract

In applications for high-T_c superconducting DC-SQUIDs such as biomagnetism, nondestructive evaluation and the relaxation of magnetic nanoparticles, it is important to maintain reliable sensor performance over an extended time period. We designed and produced DC-SQUID gradiometers based on $YBa_2Cu_3O_{7-x}$ (YBCO) thin films which are inductively coupled to a flux transformer to achieve a higher sensitivity. The gradiometers are protected against ambient atmosphere and humidity by SiO_2 and amorphous YBCO layers.

The noise properties of the sensor in flip-chip configuration, especially in unshielded environments, are shown. We present a comparison of $Tl_2Ba_2CaCu_2O_{8+x}$ (TBCCO) thin films on buffered sapphire or $LaAlO_3$ substrates for the flux transformer in shielded and unshielded environments. We reach a low white field gradient noise of 72 fT/(cm · Hz) with the TBCCO on $LaAlO_3$ flux transformer. The electric properties of the gradiometers (critical current I_C, normal state resistance R_N and the transfer function V_Φ) were measured over a period of one year and do not show significant signs of degradation.

1 Introduction

Long-term sensor stability is a requirement for the application of high temperature superconducting DC-SQUID gradiometers. Changes in the electrical characteristics of sensors lead to decreased performance and a higher cost of the final system. The most sensitive areas of the gradiometer are the Josephson junctions, which we create using a single layer bicrystal technology. An overview of the properties of grain boundary Josephson junctions is given in [1]. A possible cause for degradation of superconducting thin films is the diffusion of oxygen in the YBCO layer. In monocrystalline films the oxygen transport occurs along the a-b plane of the crystals [2]. At growth defects or grain boundaries a significant oxygen diffusion appears along the c-axis of the epitaxially grown film [3, 4]. Therefore a passivation at the sides and on top of the superconducting thin film is necessary to reduce diffusion. We developed a process to compensate for height differences during fabrication and protect our sensors using different materials to achieve stability over a period of more than one year.

2 Fabrication

The sensors described here are galvanically coupled DC-SQUID gradiometers (for layout see figure 1). The YBCO thin films having a thickness of 150 nm are grown along the c-axis on $SrTiO_3$ bicrystal substrates with pulsed laser deposition [5]. The thin films are patterned with Ar-ion beam etching and planarized *in*

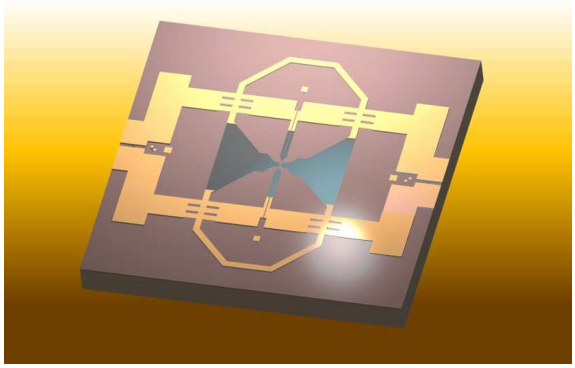

Figure 1: Schematic of the planar DC-SQUID gradiometer

situ via the deposition of 150 nm amorphous YBCO with RF-sputtering. For repeated measurements with different combinations of readout gradiometers and flux transformers the sensors need to be protected against mechanical damage and require high-quality bond contacts. The direct contact between readout gradiometer and flux transformer in the flip-chip package can lead to damages in the thin films which influence the electrical properties of the system. A protective layer is also necessary to reduce diffusion of oxygen and to avoid contact between the superconducting thin film and environmental humidity. In our current setup we use SiO_2 for this layer on the top of the YBCO film. Further details regarding the thin film system is given in [6].

We developed a new technique to prepare the the bonding pads of the sample. The aim was to improve the adhesion of the bond wire and to lower the contact resistance. Therefore, prior the YBCO deposition, we grow a 50 nm thin gold layer on the substrate using a lift-off technique. During heating of the substrate to the deposition temperature of 750°C the gold layer clusters to small islands with a diameter of $1-2$ μm (see figure 2). Between these islands the YBCO growths well c-oriented with a rocking-curve width of less than 0.3° and a critical temperature higher than 86 K. The contact resistance of an average bonding pad was lowered from 160 mΩ (without gold clusters) to < 4 mΩ (with gold clusters).

The SQUID consists of two Josephson junctions with a width of 3 μm and a galvanic coupling to the antenna structures. The pickup loops of the antenna structure are used in a gradiometric configuration. An external magnetic field gradient leads to a difference in magnetic flux in the antenna structures. This difference is galvanically coupled into the SQUID with the current ΔI (see figure 3) and an inductance of the incoupling line of the SQUID loop L_M. The length of the SQUID loop is either $l = 50$ μm or in a second layout $l = 70$ μm (see figure 3), the width of the incoupling lines is 5 μm and the inner hole area is 4 μm wide. In former investigations we have shown that for a film thickness of about 150 nm the inductance L_M of a DC-SQUID with a width of the incoupling lines of 5 μm and an inner area of 3 μm can be estimated by a factor of 1.05 pH/μm times the loop length. The decrease of the width of incoupling lines to 4 μm and the increase of the width of the inner area to 5 μm increase this factor to a value of about 1.8 pH/μm [7]. With these specifications we estimate the coupling inductance of the DC-SQUIDs in our gradiometers to be in the range of 50 pH in the ideal case, up to 90 pH for a loop length of 50 μm. The exact value depends on the accuracy of the photolithography and patterning process. To determine the coupling inductance we usually measure the flux modulation of the DC-SQUID with a current directly

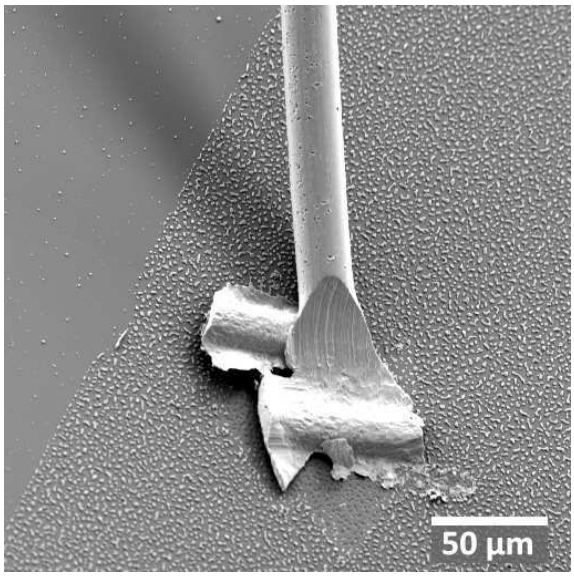

Figure 2: SEM image of a bonding pad with attached bond wire. Gold clusters provide good adhesion with low contact resistance to the YBCO film.

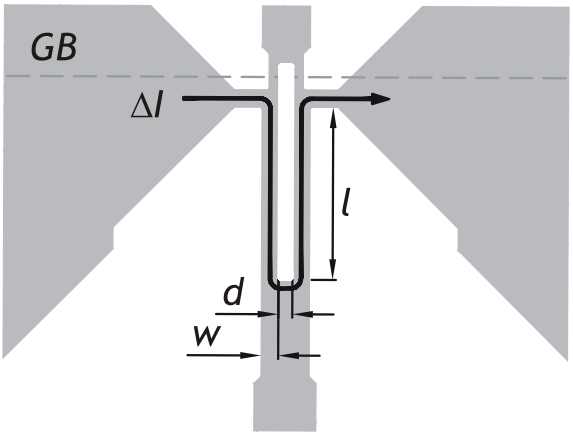

Figure 3: Inner part of the DC-SQUID gradiometer with loop length l, width of the superconducting lines w, inner loop width d and grain boundary (GB). The difference in magnetic flux is galvanically coupled into the SQUID loop with the current $\Delta I = \Delta I_F \cdot K$, with the difference current in the flux transformer ΔI_F and the coupling constant K.

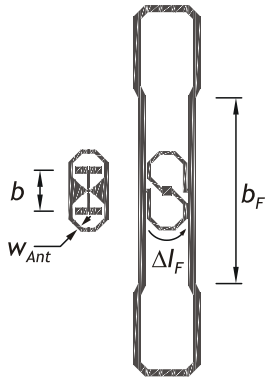

Figure 4: Flip chip configuration with readout gradiometer on the left side and flux transformer on the right side. The difference in screening currents ΔI_F is magnetically coupled into the readout gradiometer.

coupled into the SQUID loop [8]. This precise method is only possible after disconnecting the antenna structures so that these measurements can only be done after the long term experiments.

To optimize the coupling between the antenna of the readout gradiometer and the antenna of the flux transformer we used different widths W_{ant} for the antenna of the readout gradiometer (200 μm, 400 μm and 600 μm, see figure 1)[9].

The flux transformer is prepared on a separate substrate (see figure 4). We used two different substrate materials and TBCCO as the superconducting thin film material. The comparison between YBCO and TBCCO on different subtrate materials for the flux transformer has shown that TBCCO leads to the best sensor performance, i.e. the lowest white noise level, due to a better flux pinning in unshielded environment [10]. The size of the complete flux transformer is 8×40 mm^2 and the baselength b_f is 19 mm. After patterning by wet etching 300 nm of SiO_2 are deposited on the flux transformer as protection against chemical and mechanical influences. The two pickup loops of the flux transformer are connected in parallel. The current caused by a difference in magnetic flux is inductively coupled to the readout gradiometer with an S-shaped superconducting line, which is optimized to the dimensions of the readout gradiometer.

3 Electrical Characteristics

We focused our measurements on the electrical characteristics at liquid nitrogen temperatures. The sensors were evaluated over a period of one year in a magnetically shielded environment (two layers of μ-metal) to reduce the influence of external disturbances. During this period each sensor was cooled and then heated to room temperature ten times to simulate environmental stress during the normal sensor lifetime. Between the measurements the gradiometers and flux transformers were stored at room temperature with a humidity of 40–45%.

To measure their I-V characteristics, the DC-SQUID gradiometers were biased with different currents and the resulting voltage signal was amplified and recorded. With this information we calculated the critical current I_C, normal state resistance R_N and the $I_C R_N$ product (see figure 5). The $I_C R_N$ product allows to compare different types of Josephson junctions independent of the junction geometry. This parameter should change significantly if degradation between the measurements occurs. To evaluate the response to external magnetic fields we calculated the transfer function of the sensors over time (see figure 6). At a fixed bias current the maximum voltage modulation V_{pp} is measured as a function of the current

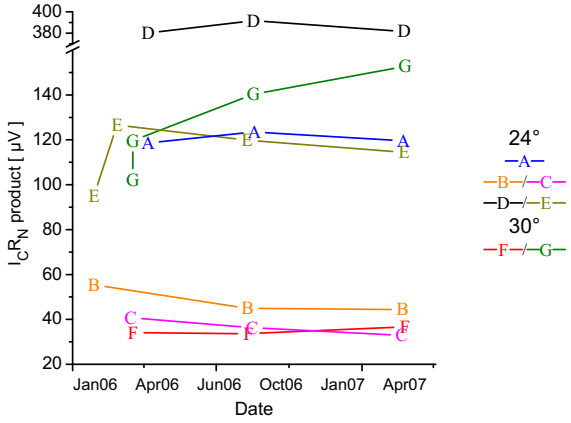

Figure 5: Time dependence of the critical current and the normal state resistance of seven readout gradiometers with grain boundary angles of 24° and 30°.

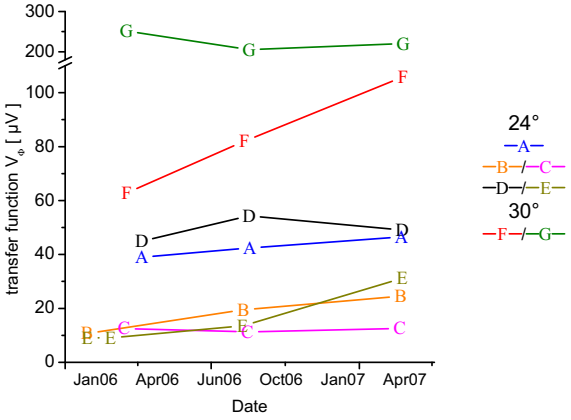

Figure 6: Time dependence of the transfer function of the readout gradiometers in figure 5.

in a small copper coil I_M. Assuming a sinusodial $V(I_M)$ characteristic the transfer function V_Φ can be calculated as $V_\Phi = \pi \cdot V_{pp}$.

4 Experimental Results

An important improvement to realize sensors with a long lifetime was the usage of SiO_2 passivation layers and amorphous YBCO films. As a first step we examined whether there is a negative influence of the passivation on the superconducting properties of the sensors. With all tested sensors the SiO_2 thin film did not change the electrical characteristics and the dielectric influence is negligible compared to the influence of the substrate material ($SrTiO_3$).

The planarisation of the structures with amorphous YBCO deposited by hollow cathode sputtering does not lead to a large change of the superconducting properties of bicrystal Josephson junctions. In some cases we observed a slight increase of the critical current, compared to bicrystal junctions without planarisation. This can be caused by oxygen diffusion between the planarisation layer consisting of $YBCO_{7-x}$ with $x \approx 0$ and the crystalline thin film with $0.1 > x > 0$. An increase of the critical current is primarily observed for bicrystal angles of 30° and above.

During the the processing of the gradiometer, especially during the dry etching and photolithography steps a temperature increase of the thin film up to 100°C accelerates the diffusion of oxygen into the area of the Josephson junctions instead of out of this area as observed without amorphous YBCO planarisation thin films. To lower the rate of diffusion out of the antenna areas the substrate is cooled by liquid nitrogen during the dry etching procedure [11, 12].

The comparison among gradiometers (see figure 5) shows a large spread of the $I_C R_N$ product due to different current densities of the grain boundary junctions used for these experiments. All of these junctions show the typical scaling behaviour for grain boundary junctions [10]. Compared to previous experiments by other groups only the $I_C R_N$ value of 30 μV for the 30° grain boundary junction (curve F) is relatively low [13]. The experimental investigations of the long term stability shows no relevant changes or signs of degradation in most cases (see figure 5). Only small changes of the $I_C R_N$ product were measured. In all of these cases the reason for this behaviour was a decrease of the respective critical current. A decreasing I_C does not automatically lead to a decrease in the transfer function, as aging processes can change R_N at the same time.

The 24° and 30° grain boundary junctions used in our experiments exhibit relatively high critical current densities. In combination with a width of the SQUID structures in the range of 3 μm the critical currents can be as high as 100 μA. With high critical currents the inductance parameter β_L can exceed the optimum value (≤ 1), which leads to a decreasing transfer function [8, 14]. Higher β_L values reduce the voltage modulation due to a screening of the flux which is coupled into the SQUID. Therefore a slight decrease of the critical current results in an improvement of the transfer function (sample B and E). Such a decrease can be caused by diffusion during the processing of the superconducting thin film or by slower diffusion during normal operation of the sensor.

In the case of increasing critical current (sample G) we see a reduction of the transfer function V_Φ in figure 6. In our experiments the transfer function increased significantly for only one sample with a 30° grain boundary (sample F); the reason for this is topic of future investigations.

The fabricated gradiometers display a large spread in the transfer function with a minimum of 10 μV. However, all sensors were able to operate in unshielded environment with commercially available SQUID electronics (Magnicon, Philips).

In the next step we have measured various combinations of readout gradiometers and flux transformers

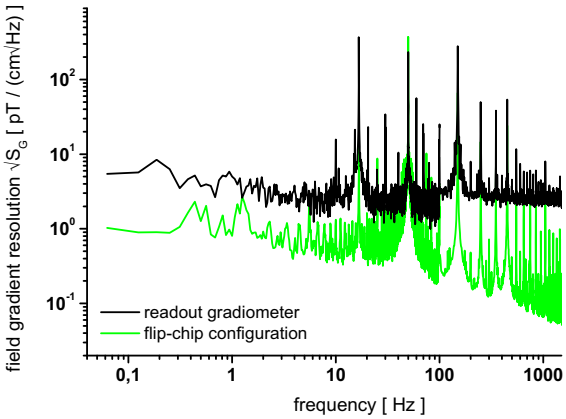

Figure 7: Field gradient resolution of the readout gradiometer without and with flux transformer.

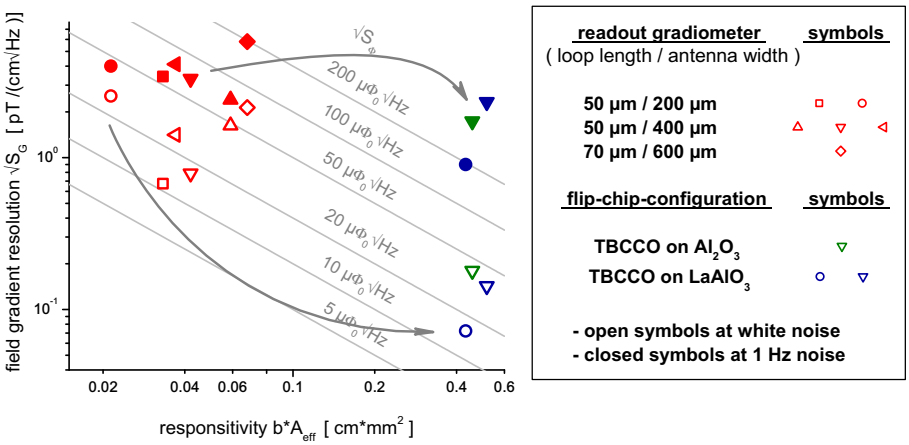

Figure 8: Field gradient resolution over responsitivity in magnetically unshielded environment with readout gradiometer on the left side and flip-chip configuration on the right side.

in shielded as well as in unshielded environment [10]. The field gradient resolution $\sqrt{S_G}$ is proportional to the flux noise $\sqrt{S_\Phi}$ and depends on the effective area of the configuration A_{eff} and the base length b:

$$\sqrt{S_G} = \frac{\sqrt{S_\Phi}}{b \cdot A_{eff}} \tag{1}$$

The responsitivity of a gradiometer is defined as the product of effective area and base length. Figure 7 shows as an example the increase of the field gradient resolution in unshielded environment for the readout gradiometer (sample G) in comparison to the flip chip configuration. Due to the large flux transformer the flip chip configuration with a higher base length ($b_f \approx 1.9$cm) and an increased effective area ($A_{eff} \approx 0.22\text{mm}^2$)

The field gradient resolution as a function of the responsitivity for different read out gradiometers at 1 Hz and white noise region is illustrated in figure 8. By changing the width of readout gradiometer antenna w_{ant} the responsitivity can be adjusted but the field gradient resolution is mostly unchanged. The reason

for this behaviour is the higher flux noise in unshielded environment for larger antenna widths. Especially the largest incoupling inductance L_M (loop length $l = 70$ μm) together with the largest antenna width results in the largest responsitivity (> 0.06 cm $\cdot$ mm^2, $\diamond$), but leads to a relatively low field gradient resolution in unshielded environment, caused by the large flux noise of 200 $\mu\Phi/\sqrt{\text{Hz}}$ in comparison to the lower value of about 50 $\mu\Phi/\sqrt{\text{Hz}}$ for the other gradiometer layouts.

This means that, for the development of sensors in flip chip configuration, it can be helpful to optimize the readout gradiometers in the direction of low flux noise in unshielded environment, not in the direction of higher responsitivity. As in the same figure shown we realized the best value in the field gradient resolution with the readout gradiometer with the lowest level in the flux noise (< 50 $\mu\Phi/\sqrt{\text{Hz}}$, $l = 50$ μm, 200 μm line width, $\circ$) in unshielded environment not with the sensor with the higher responsitivity (0.04 cm $\cdot$ mm^2). If the readout gradiometer alone has a large responsitivity ($A_{eff} \cdot b$) the additional flux transformer only improves the field gradient resolution by a factor of two.

With a similar flux noise, it should be possible to reduce the field gradient resolution significantly due to the higher responsitivity of the combination of readout gradiometer and flux transformer. We are able to achieve a reduction by a factor of 5, corresponding to a field gradient resolution of 880 fT/(cm$\sqrt{\text{Hz}}$) at frequencies around 1 Hz and a reduction by a factor of 20 (72 fT/(cm$\sqrt{\text{Hz}}$)) at higher frequencies, showing the effectiveness of this approach.

5 Summary

The developed and fabricated sensors were successfully protected by a combination of an amorphous YBCO and SiO_2 layers against oxygen diffusion. After a period of one year no significant signs of degradation were detected.

With TBCCO flux transformers on $LaAlO_3$ substrates stacked with readout gradiometers, we achieve a field gradient noise of 72 fT/(cm$\sqrt{\text{Hz}}$) for the white noise level and 880 fT/(cm$\sqrt{\text{Hz}}$) at 1 Hz in unshielded environments. We are continuing to investigate the stability over longer time periods and include the noise investigations in shielded as well as unshielded environment.

Acknowledgment

The authors would like to thank L. Redlich (IPHT Jena) for laser patterning of the grain boundary markers of the samples. This work is partially supported by EU BIODIAGNOSTICS (017002).

References

[1] Gross R 2005 *Physica C* **432** 105–115

[2] Aarnink W A M, Ijsselsteijn R P J, Gao J, van Silfhout A and Rogalla H 1992 *Phys. Rev. B* **45** 13002–13007

[3] Kittelberger S, Bolz U, Huebener R P, Holzapfel B and Mex L 1998 *Physica C* **302** 93–101

[4] Tian Y J, Linzen S, Schmidl F, Matthes A, Schneidewind H and Seidel P 1999 *Thin Solid Films* **338** 224–230

[5] Seidel P, Schmidl F, Wald H, Mans M, Peiselt K, Baldeweg U, Beck M, Biering S, Becker C, Uhlig J and Grosse V 2005 *IEEE Trans. Appl. Supercond.* **15** 161–164

[6] Seidel P, Becker C, Steppke A, Foerster T, Wunderlich S, Grosse V, Pietzcker R and Schmidl F 2007 *Physica C* In press

[7] Schmidl F, Wunderlich S and Seidel P 2001 *High-T_c Superconductors and Related Materials* (*NATO Science Series 3. High Technology* vol 86) (Boston: Kluwer Acadamic Publishers Group) chap Design of HTS DC SQUID gradiometer for application in nondestructive evaluation and biomagnetism, pp 535–552

[8] Wunderlich S, Schmidl F, Dörrer L, Schneidewind H and Seidel P 1999 *IEEE Trans. Appl. Supercond.* **9** 71–76

[9] Peiselt K, Schmidl F, Linzen S, Anton A S, Hübner U and Seidel P 2003 *Supercond. Sci. Technol.* **16** 1408–1412

[10] Seidel P, Foerster T, Schneidewind H, Becker C, Grosse V, Steppke A, Lorenz P, Pietzcker R and Schmidl F 2007 *IEEE Trans. Appl. Supercond.* In press

[11] Schneidewind H, Schmidl F, Linzen S and Seidel P 1995 *Physica C* **250** 191–201

[12] Alff L, Fischer G M, Gross R, Kober F, Beck A, Husemann K D, Nissel T, Schmidl F and Burckhardt C 1992 *Physica C* **200** 277–286

[13] Minotani T, Kawakami S, Kiss T, Kuroki Y and Enpuku K 1997 *Jpn. J. Appl. Phys.* **36** L1092–L1095

[14] Wunderlich S, Redlich L, Schmidl F, Dörrer L, Köhler T and Seidel P 2000 *Physica C: Superconductivity* **340** 51–64